

# Negative Refraction and Superresolution Using Transparent Metallo-Dielectric Stacks

Michael Scalora<sup>1</sup>, Giuseppe D'Aguanno<sup>1</sup>, Neset Akozbek<sup>2</sup>, Marco Centini<sup>3</sup>,  
Domenico de Ceglia<sup>1,4</sup>, Mirko Cappeddu<sup>1,5</sup>, Nadia Mattiucci<sup>2</sup>, Joseph W. Haus<sup>6</sup>,  
Mark J. Bloemer<sup>1</sup>

*1 Charles M. Bowden Research Center, AMSRD-AMR-WS-ST, RDECOM,  
Redstone Arsenal, AL 35898-5000*

*2 Time Domain Corporation, Cummings Research Park 7057 Old Madison Pike  
Huntsville, Alabama 35806, USA*

*3 INFN at Dipartimento di Energetica, Universita di Roma 'La Sapienza', Via A.  
Scarpa 16, 00161 Roma, Italy*

*4 Dipartimento di Elettrotecnica ed Elettronica, Politecnico di Bari, Via Orabona 4,  
70124 Bari, Italy*

*5 Universita' degli Studi di Catania, Dipartimento di Ingegneria Elettrica Elettronica e  
dei Sistemi, Via A. Doria 6, 95125 Catania - Italy*

*6 Electro-Optics Program, University of Dayton, Dayton, OH 45469-0245, USA*

## ABSTRACT

Negative refraction is known to occur in materials that simultaneously possess a negative electric permittivity and magnetic permeability; hence they are termed negative index materials. However, there are no known natural materials that exhibit a negative index of refraction. In large part, interest in these materials is due to speculation that they could be

used as perfect lenses with superresolution. We propose a new way of achieving negative refraction with currently available technology, based on transparent, metallo-dielectric multilayer structures. The advantage of these structures is that both tunability and transmission (well above 50%) can be achieved in the visible wavelength regime. We demonstrate both negative refraction and superresolution in these structures. Our findings point to a simpler way to fabricate a material that exhibits negative refraction. This opens up an entirely new path not only for negative refraction, but also to expand the exploration of wave propagation effects in metals.

The propagation of light inside metals has never been seriously considered because bulk metals are highly opaque at almost all wavelengths across the entire electromagnetic spectrum. A quasi-transparent region naturally occurs near the so called plasma frequency, where the real part of the index of refraction approaches unity, and absorption is minimized [1]. Understanding the propagation of light in metals has taken on a special significance since the prediction that an object, illuminated with TM-polarized light, may form a super-resolved image of itself on the other side of the barrier [2]. The image is formed by negative refraction [3] that occurs inside the metal, which focuses a diverging wave-front (the beam) down to a very tight spot, thus exciting large spectral components (k-space), including evanescent modes. The argument made is that the presence of evanescent modes at the focus, in addition to the propagating modes, makes it possible for the image to be resolved beyond the limits imposed by ordinary optical materials and by diffraction [2].

The basic mechanism described in reference [2] is based on a change in direction of the longitudinal component of the electric field inside the metal, which fosters a change in direction of the Poynting vector. In other words, the Poynting vector of a TM-polarized beam, incident at an angle on a metal surface, or layer, *refracts* evanescently with a negative angle inside the metal. We italicize the word "refracts" because the Poynting vector  $\mathbf{S}$  and the wave vector  $\mathbf{k}$  are not co-directional. It is the continuity of the longitudinal component of the electric displacement field,  $\mathbf{D}=\epsilon\mathbf{E}$ , at the boundary that forces the change in the direction of propagation of the Poynting vector. Then, if the metal is sufficiently thick, and the object is sufficiently close, the rays may converge twice, once inside the metal layer, and a second time outside it, where the object is

imaged with features that exceed the diffraction limit, i.e. superresolution. The effect predicted in reference [2] has been experimentally observed and verified [4, 5].

A shortcoming with the single-layer super-lens is the opacity of metals. Therefore, theoretical predictions were made, and experiments carried out, using silver layers approximately 40nm or less, above but near the plasma frequency, which occurs at  $\sim 320$ nm, where the dielectric constant of silver is negative, and the material is still somewhat transparent. The modus operandi of the transmission process is based on the excitation of surface modes, which evanescently couple the light to the other side of the barrier. In general, transmittance is rather low, typically not exceeding a few percent [4, 5], but the transmission may be increased somewhat by placing sub-wavelength holes on the metal sheet [6]. The opacity of metals has thus driven researchers to seek negative refraction and super-lensing in a roundabout way, by first engineering a negative index material in the microwave regime using metallic rods and loops to induce an electric and magnetic resonance [7-9], and then by seeking a way to scale down the size of magnetic circuits using nano-wires or nano-strips, for example, in order to access the much coveted visible region [10]. However, the containment of material and scattering losses, along with the successful achievement of size reduction, remain formidable challenges.

In this article we report that there is a relatively easy way to obtain negative refraction for TM-polarized light throughout the visible range, using so-called transparent metals [11-14]. These are layered, metallo-dielectric stacks that may contain several metallic layers, where the thickness of each layer may be tens of nanometers, so that total metal thickness may easily reach into the hundreds of nanometers. Remarkably, the structure can be designed so that it remains transparent within pre-selected, broad

wavelength ranges in the visible region and beyond. The location of the transparency window usually depends on the thickness of the intervening dielectric material, and can be engineered rather easily by using a combination of appropriate metals, and/or dielectric materials, from the visible well into the mid-infrared range. For instance, one may use almost any dielectric or semiconductor material, in combination with aluminum (for work in the ultraviolet range), silver (best used in the visible part of the spectrum), gold, and copper (both better suited for near-infrared applications). As an example, an 11-layer, Ag/MgF<sub>2</sub> stack containing 150nm of silver was fabricated [12, 13] using thermal evaporation techniques, that featured a peak transmittance of about 52% at 532nm, with a full width at half maximum well in excess of 100nm. Metal layer thicknesses ranged from a low of 25nm, to a high of 40nm, and so it is possible to further increase transmittance by thinning out Ag layers, and by choosing a material with a relatively high index of refraction, such as ZnO or TiO<sub>2</sub> [14]. We note that an approach that considers infinitesimally thin, metallo-dielectric multilayers for negative refraction has been considered previously [15]. However, the approach is not an interferometric one, relies on evanescent wave coupling, does not achieve nearly the same transparencies, and so it fails in the regime we are considering because it assumes that each metal layer is so thin that it forms a nano-sheet, and the stack may be thought of as an effective medium characterized by an average dielectric susceptibility and a mean-field.

To present our results we use a pulse propagation model that integrates the vector Maxwell's equations in the time domain with two spatial coordinates and time. The model is described in detail elsewhere, and it was derived for the general conditions of dispersive and discontinuous dielectric susceptibility and magnetic permeability

[14,16,17]. Our typical scenario unfolds within a structure roughly 500nm thick, half of which may be metal. Assuming a TM-polarized incident field with the magnetic field polarized in the x-direction, using the model we may calculate any electromagnetic quantity of interest. For example, the Poynting vector takes the form:

$$\begin{aligned} \mathbf{S} &= \frac{c}{4\pi} \mathbf{E} \times \mathbf{H} = \hat{\mathbf{z}} S_{\xi}(\tilde{y}, \xi, \tau) + \hat{\mathbf{y}} S_{\tilde{y}}(\tilde{y}, \xi, \tau) \\ &= \frac{c}{4\pi} \left( -\hat{\mathbf{z}} (\Im \mathcal{C}_x \mathcal{E}_{\tilde{y}}^* + \Im \mathcal{C}_x^* \mathcal{E}_{\tilde{y}}) + \hat{\mathbf{y}} (\Im \mathcal{C}_x \mathcal{E}_{\xi}^* + \Im \mathcal{C}_x^* \mathcal{E}_{\xi}) \right) \end{aligned} \quad (1)$$

All fields represent complex, general envelope functions. The total momentum is then defined as follows:

$$\begin{aligned} \mathbf{P}(\tau) &= P_{\tilde{y}}(\tau) \hat{\mathbf{y}} + P_{\xi}(\tau) \hat{\mathbf{z}} \\ &= \hat{\mathbf{y}} \int_{\xi=-\infty}^{\xi=\infty} \int_{\tilde{y}=-\infty}^{\tilde{y}=\infty} \mathbf{g}_{\tilde{y}}(\tilde{y}, \xi, \tau) d\tilde{y} d\xi + \hat{\mathbf{z}} \int_{\xi=-\infty}^{\xi=\infty} \int_{\tilde{y}=-\infty}^{\tilde{y}=\infty} \mathbf{g}_{\xi}(\tilde{y}, \xi, \tau) d\tilde{y} d\xi \end{aligned} \quad (2)$$

where  $\mathbf{g}_{\xi, \tilde{y}}(\tilde{y}, \xi, \tau) = \frac{\mathbf{S}_{\xi, \tilde{y}}(\tilde{y}, \xi, \tau)}{c^2}$  is the Abraham electromagnetic momentum density.

In addition, the Snell or refraction (phase front) angle is calculated as the expectation value of the vector sum of the individual wave vectors along the two spatial coordinates:

$$\langle \mathbf{k}(\tau) \rangle = \int_{k_{\xi}=-\infty}^{k_{\xi}=\infty} \int_{k_{\tilde{y}}=-\infty}^{k_{\tilde{y}}=\infty} \left( \hat{\mathbf{y}} k_{\tilde{y}} + \hat{\mathbf{z}} k_{\xi} \right) |H(k_{\tilde{y}}, k_{\xi}, \tau)|^2 dk_{\tilde{y}} dk_{\xi} \quad (3)$$

Although for individual plane waves the direction of the Poynting vector coincides with the direction of the electromagnetic momentum density, for localized wave packets it is always more appropriate to talk about momentum. As defined in Eqs.(1-3), one generally finds that  $\mathbf{P}$  and  $\mathbf{k}$  are co-directional in ordinary, isotropic, low-absorption materials, and that in negative index materials they point in opposite directions [15], as expected [3].

Eqs.(1-3) represent instantaneous quantities. Taken together they may be used to

calculate the refraction angles of both momentum (or energy) and phase front. As mentioned earlier, we use the word "refraction" with some caution, because it is usually intended to mean the direction of the wave vector  $\mathbf{k}$ . However, this parallelism ceases to hold in metals, for both TE and TM polarized incident waves. The consequences are more dramatic in the case of TM polarized fields, because they lead to anomalous refraction of the Poynting vector, as discussed in reference [2].

To illustrate the negative refraction process through a transparent metal stack, we examine the propagation of short pulses through a 6 and 1/2 period, Ag(25nm)/X(22nm) stack. Here, X represents a generic, high index material that we use to show how the process works, and at the end we will provide a list of suitable materials. We assume the index of refraction of material X is  $n=4$ . The stack contains 150nm of silver metal, and it is approximately 282nm thick. The first and last layers of the stack are X layers, each approximately 11nm thick. This choice is useful because it tends to smooth and maximize the transmission function, and to minimize reflections [14]. In Fig.1 we depict the plane-wave transmittance through the stack as a function of wavelength, for TM-polarized light incident at  $45^\circ$ . We first tune the carrier wavelength of the incident pulse at 400nm, where the transmittance is  $\sim 43\%$ . The dielectric constant of Ag at 400nm is  $\epsilon = -3.77 + i0.67$  [1]. We note that we use actual material data because we find that it is important to do so if one is to seek both qualitative and quantitative agreement with experiments [12, 13]. For simplicity, but only for the moment, we assume that material X is dispersionless and absorptionless.

We assume our incident pulse is Gaussian, and  $\sim 15$  fs in duration, with carrier frequency tuned to 400nm. Fig.(2) contains several snapshots that chronicle the

dynamics of the pulse as it traverses the stack. The centroid of the transmitted wave packet appears to be shifted upward, a detour that is best perceived for short, well-localized wave packets, but that clearly holds for pulses of larger spatial extension and longer duration. This shift can only be understood in terms of additional upward momentum supplied to the pulse by the structure.

Fig.(3) summarizes the negative refraction process and our basic result. Although the quantities we calculate are instantaneous, one may proceed by either performing a time average as the pulse dwells inside the stack, or by simply taking the most dominant values, which occur when the peak of the pulse arrives at the structure. The total momentum refracts anomalously inside the transparent metal stack, forming an angle of approximately  $-25^\circ$  with the normal. Given a structure length of 282nm, the upward shift, denoted by  $\delta$  in the figure, is given by  $\delta \sim 131\text{nm}$ . Furthermore, calculations similar to those exemplified in Fig.(2) were carried out for incident angles of  $30^\circ$  and  $60^\circ$ . The resulting *momentum* refraction angles were found to be  $\sim -17^\circ$  and  $\sim -31^\circ$ , respectively. Application of Snell's law immediately reveals that all these angles have in common an *effective*, negative refractive index of  $n \sim -1.67$ . The reality is, of course, somewhat more complicated, but the result is rendered even more dramatic by the fact that total momentum and total wave vector *do not* point in the same direction, and in fact in this case they point in altogether different quadrants. Yet, Snell's law appears to still point the wave in the right direction. Of course, one cannot ascribe to the wave vector its usual meaning and qualities, and a clear inequality between group and energy velocity quickly emerges, with the group velocity becoming an ill-defined concept.

Although this result may seem surprising, the fact is that energy and group

velocities are the same only for homogenous media, away from any boundaries [18]. It has already been demonstrated that, in the absence of absorption, the two velocities are generally different near surfaces or inside strongly scattering one-dimensional systems, such as photonic band gap structures of finite size [19]. This discrepancy is associated with pulse reshaping and scattering losses due to geometrical dispersion, i.e. the introduction of longitudinal index discontinuities. Nevertheless, the physical difference between group and energy velocity is generally not recognized even in structures of finite length, and in most of the literature the terms are inappropriately used interchangeably. Then, it should not be surprising to discover that in absorbing, two-dimensional systems such as ours energy and group velocities cease also to be collinear, and not quite so easily related. A study of the Fourier spectrum of the pulse, similar to that done in reference [16], clearly shows that all spectral components develop in a way that  $\langle \mathbf{k} \rangle$  and  $\mathbf{P}$  point in opposite quadrants.

Now that we have established that negative refraction occurs in the visible range, we wish to test the structure's performance across the transparency window. We fix the incident angle at  $45^\circ$ , tune the carrier frequency of the pulse at 500nm, and find a negative refraction angle of  $\sim -13^\circ$ . We then tune the pulse at 600nm, and find that the pulse still refracts negatively, but with an angle of approximately  $-1^\circ$ . Although the basic cause and effect for the pattern that emerges is quickly identified, namely that the magnitude of the dielectric constant of silver eventually overtakes that of the dielectric material ( $\epsilon=16$ ) at longer wavelengths, more is at play here than just a simple ratio of dielectric constants. First, let us recall our stated need for a high index material. At 400nm, the magnitude of the ratio between the real parts of the dielectric constant is

16/3.77. At 500nm the ratio drops to 16/8.57, and by the time we reach 600nm the ratio is  $\sim 16/14$ . The refraction process is generally anomalous (upper, right quadrant) in each metal layer, and normal (lower, right quadrant) in each dielectric layer. This aspect of the dynamics is exemplified on the right side of Fig.(3), where we show the momentum vectors in each type of layer. The higher index of refraction accomplishes at least two things inside the dielectric layers: it keeps the ray closer to the normal (smaller refraction angle), and it slows down the wave. At the same time, and perhaps more importantly, the electric fields become localized inside the metal layers in almost equal measure compared to the dielectric layers [11-14].

In bulk metals, the electric and magnetic fields are out of phase by approximately  $45^\circ$  [17], as the electric field is expelled from the metal. This phase mismatch translates into a spatial delocalization of the fields. In sharp contrast, inside our transparent metal stack this spatial delocalization does not hold, as both electric and magnetic fields simultaneously occupy each metal layer. In fact, the magnetic field has local maxima inside the metal. As a result, and in addition to pointing in the anomalous direction, the local Poynting vector (and resulting momentum), which is the product of the electric and magnetic fields, can be large inside the metal. When this is combined with the fact that the dielectric momentum makes a shallower angle with the normal, then the metal-momentum dominates to yield a total momentum that points in the anomalous direction. These dynamics are completely determined by an interference phenomena that generally requires relatively thick metal layers, unlike the approach outlined in reference [15], (thinner layers may improve transparency, but also reduce the amount of anomalous, upward momentum), and takes advantage of field localization inside the metal layers in

such a way that cannot otherwise be accomplished in any single, metallic layer.

Up to this point we have only addressed the issue of the existence of negative refraction. However, we also wish to tackle the subject of super-lensing, and whether it is possible to resolve an object below the wavelength limit. We begin by once again considering a pulse tuned at 400nm, but this time it is incident on a metal shield with a small aperture. The metal shield is approximately 180nm thick, opaque by any measure, but we carve out a small slit approximately  $0.25\mu\text{m}$  across. The situation is exemplified in Fig.(4). The slit is located approximately 50nm away from the stack, and the image plane is located approximately 600nm away from the slit, or  $\sim 300\text{ nm}$ , less than one wavelength, away from the stack. The field transmitted through the slit is sampled at different times, as it propagates through the transparent metal lens. Fig.(5) captures a snapshot of the field, just as part of the wave packet forms a clear focus on the right side of the stack. The approximate center of the focus is intersected by the imaging plane (dotted line). We thus sample the field along the dotted line, and plot the resulting transverse field profile in Fig.(6). The result is a typical diffraction pattern, but the slit's image casts a bright, discernable spot, with full width at half maximum (FWHM) of approximately  $0.16\mu\text{m}$ , which resolves the slit with an incident wavelength approximately four times larger. In comparison, in Fig.(6) we also show the transverse profile of a field diffracting from the same slit, located the same distance away from the screen. The FWHM of the freely diffracting pulse is approximately ten times broader.

The only issue that remains unresolved is the question of suitable materials. We have identified several candidates that are suitable in the visible range, for example Si, GaP, and GaAs. The indices of refraction of Si and GaAs are above 4, while that of GaP

is between 3 and 4. Although bulk Si and GaAs are opaque in the visible range, a number of thin layers may be combined with varying thicknesses of Ag to yield a transparency range. For instance, we find that 6 and 1/2 periods of Ag(32nm)/Si(22nm) yield a transmittance window centered around 500nm (where the real part of the dielectric constant of Si is  $\sim 18$ ), with maximum transmittance of  $\sim 20\%$ . At this wavelength, our model yields a negative refraction angle of  $\sim -10^\circ$ . Even though GaP has a lower index of refraction than Si, one may obtain substantially similar results (refraction angle of  $\sim -13^\circ$ , and  $n \sim -2.3$ ) by making the structure somewhat thicker. Finally, at 632nm we find that the transmittance from a 6 and 1/2 period Cu(32nm)/Si(43nm) is still approximately 30%, and yields a negative refraction angle of  $\sim -3^\circ$ . So, it is possible to find relatively common materials, and have negative refraction and super-resolution occur in the visible range.

In conclusion, we have presented theoretical evidence that negative refraction can occur throughout the visible range in transparent, metallo-dielectric, photonic band gap structures. These structures may contain hundreds of nanometers of metal, and yet they can be transparent to visible light. Our simulations suggest that incident TM-polarized waves undergo negative refraction, and that the stack may form a super-resolved image. These results open a new point of view, and may help pave the way to the achievement of practical devices and applications based on negative refraction. Since transparent metal structures have already been fabricated in the visible spectrum using a number of different dielectric materials, the experimental realization of negative refraction in such structures presents no new discernable technical challenges. Taken together with the tunable aspects of the process, which we have touched upon, the search for suitable, high-

index materials may yield candidates that could also make it possible to increase the object-lens distance. Furthermore, by searching for suitable materials, possibly with negative dielectric constant, super-resolution can be expected at longer wavelengths, with significant applications to IR imaging.

## References

- [1] Palik, E. D. Handbook of Optical Constants of Solids (Academic Press, New York, 1985).
- [2] Pendry, J. B. Negative refraction makes a perfect lens, *Physical Review Letters* **85**, 3966 (2000).
- [3] Veselago, V.G. Electrodynamics of substances with simultaneously negative electrical and magnetic permeabilities, *Sov. Phys. USPEKHI* **10**, 509 (1968).
- [4] Melville, D. O. S., and Blaikie, R. J. Super-resolution imaging through a planar silver layer *Optics Express* **13**, 2127 (2005).
- [5] Fang, N., Lee, H., Sun, and Zhang, C. X. Sub-diffraction-limited optical imaging with a silver superlens, *Science* **308**, 534 (2005).
- [6] Ebbesen, T.W., Lezec, H.J., Ghaemi, H.F., Thio, and T., Wolff, P.A. *Nature* **391**, 667 (1998).
- [7] Pendry, J.B., Holden, A.J., Robbins, D.J., and Stewart, W.J. Magnetism from conductors and enhanced nonlinear phenomena, *IEEE Transactions On Microwave Theory And Techniques* **47**, 2075 (1999).
- [8] Shelby, R.A., Smith, D.A., and Schultz, S. Experimental verification of a negative index of refraction, *Science* **292**, 77 (2001).

- [9] Parazzoli, C. G., Greigor, R.B., Li, K., Koltenbah, B.E.C., and Tanielian, M. Experimental verification and simulation of negative index of refraction using Snell's law, *Physical Review Letters* **90**, 107401 (2003)
- [10] Shalaev, V. M., Cai, W., Chettiar, U. K., Yuan, H-K, Sarychev, A. K., Drachev, V. P., and Kildishev, A. V., Negative index of refraction in optical metamaterials, *Optics Letters* **30**, (2005).
- [11] Scalora, M., Bloemer, M. J., Manka, A. S., Pethel, S. D., Dowling, J. P., and Bowden, C. M., *Journal of Applied Physics* **83**, 2377 (1998)
- [12] Bloemer, M. J., and Scalora, M. Transmissive Properties of Ag/MgF<sub>2</sub> Photonic Band Gaps, *Applied Physics Letters* **72**, 1676 (1998).
- [13] Scalora, M., Bloemer, M.J., and Bowden, C. M. Laminated photonic band structures with high conductivity and high transparency: Metals under a new light, *Optics & Photonics News*, September 1999 **10**, 23 (1999).
- [14] Scalora, M., Mattiucci, N., D'Aguanno, G., Larciprete, M.C., and Bloemer, M. J. Nonlinear pulse propagation in one-dimensional metal-dielectric multilayer stacks: Ultrawide bandwidth optical limiting, *Physical Review E* **73**, 016603, (2006).
- [15] Ramakrishna, S. A., Pendry, J.B., Wiltshire, M. C. K. , and Stewart, W. J. Imaging the near field, *Journal of Modern Optics* **50**, 1419 (2003).
- [16] Scalora, M., D'Aguanno, G., Mattiucci, N., Bloemer, M.J., Haus, J.W., and Zheltikov, A.M. Negative refraction of ultrashort electromagnetic pulses, *Applied Physics B* **81**, 393 (2005).
- [17] Scalora, M., D'Aguanno, G., Mattiucci, N., Akozbek, N., Bloemer, M.J., Centini, M., Sibilìa, C., and Bertolotti, M. Pulse propagation, dispersion, and energy in negative

index materials, Physical Review E **72**, 066601 (2005).

[18] Yariv, A., Yeh, P., Optical Waves in Crystals, (Wiley, New York, 1984).

[19] D'Aguanno G., Centini, M., Scalora, M., Sibilìa, C., Bloemer, M.J., Bowden, C.M., Haus, J.W., and Bertolotti, M., Group velocity, energy velocity, and superluminal propagation in finite photonic band-gap structures, Phys. Rev. E **63**, 036610 (2001).

[20] Jackson, J.D. Classical Electrodynamics, 2nd edition, (Wiley, New York, 1975).

### Figure Captions

**Figure 1.** Transmittance vs wavelength from a 6 and 1/2 period stack composed of Ag(25nm)/X(22nm), inclusive of entry and exit X layers 11nm thick. The angle of incidence is 45°. The transmission window extends over the entire visible range.

**Figure 2.** An incident Gaussian, TM-polarized wave packet is incident on the transparent metal stack of Figure 1. The pulse that exits to the right of the stack is shifted upward by approximately 131nm.

**Figure 3.** Schematic representation of the refraction that occurs inside the stack (left drawing). Although  $\mathbf{P}$  and  $\mathbf{k}$  point in different directions, the angle of refraction is still predicted by Snell's law. Right drawing: the local momenta inside two adjacent metal and dielectric layers are shown.

**Figure 4.** A Gaussian wave packet is incident from the left on a metal shield with an aperture  $F=0.25\mu\text{m}$  across. The transparent metal stack described in the caption of Figure 1 is located a distance  $b=50\text{nm}$  away from the slit. An image plane stands approximately  $L=0.6\mu\text{m}$  from the aperture.

**Figure 5.** Contour diagram of a snapshot of the field inside and to the right of the transparent metal stack. The figure shows that a focal point is visible just to the right of the stack, about 300nm away from it. The dotted line intersects the focus, and represents the position of an imaging plane.

**Figure 6.** Image produced by the slit on the image plane indicated on Figure 5. The full width at half maximum of the field that propagates through the stack (solid line) is approximately ten times narrower than the field emanating from the same aperture, and propagating in free space.

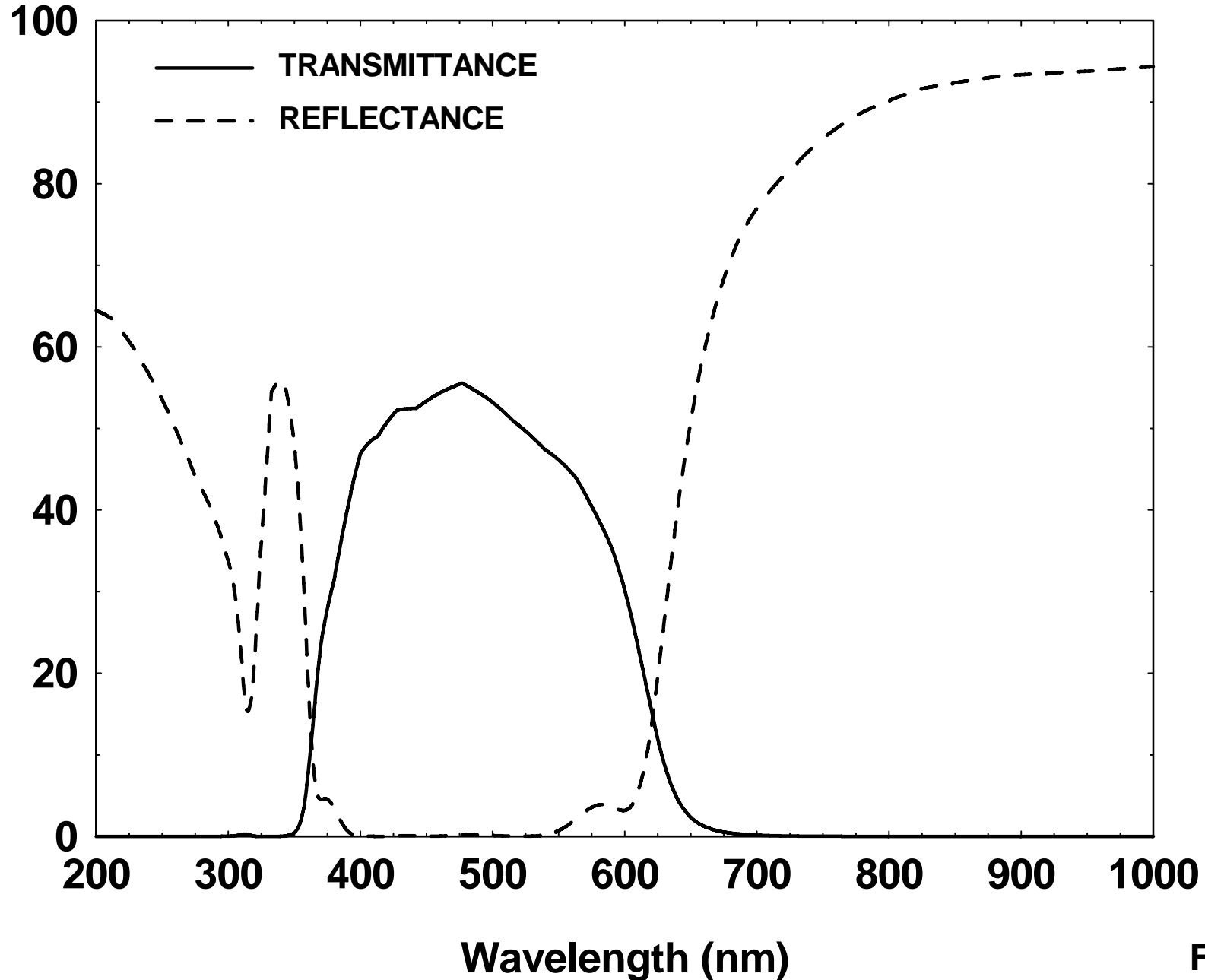


Fig.1

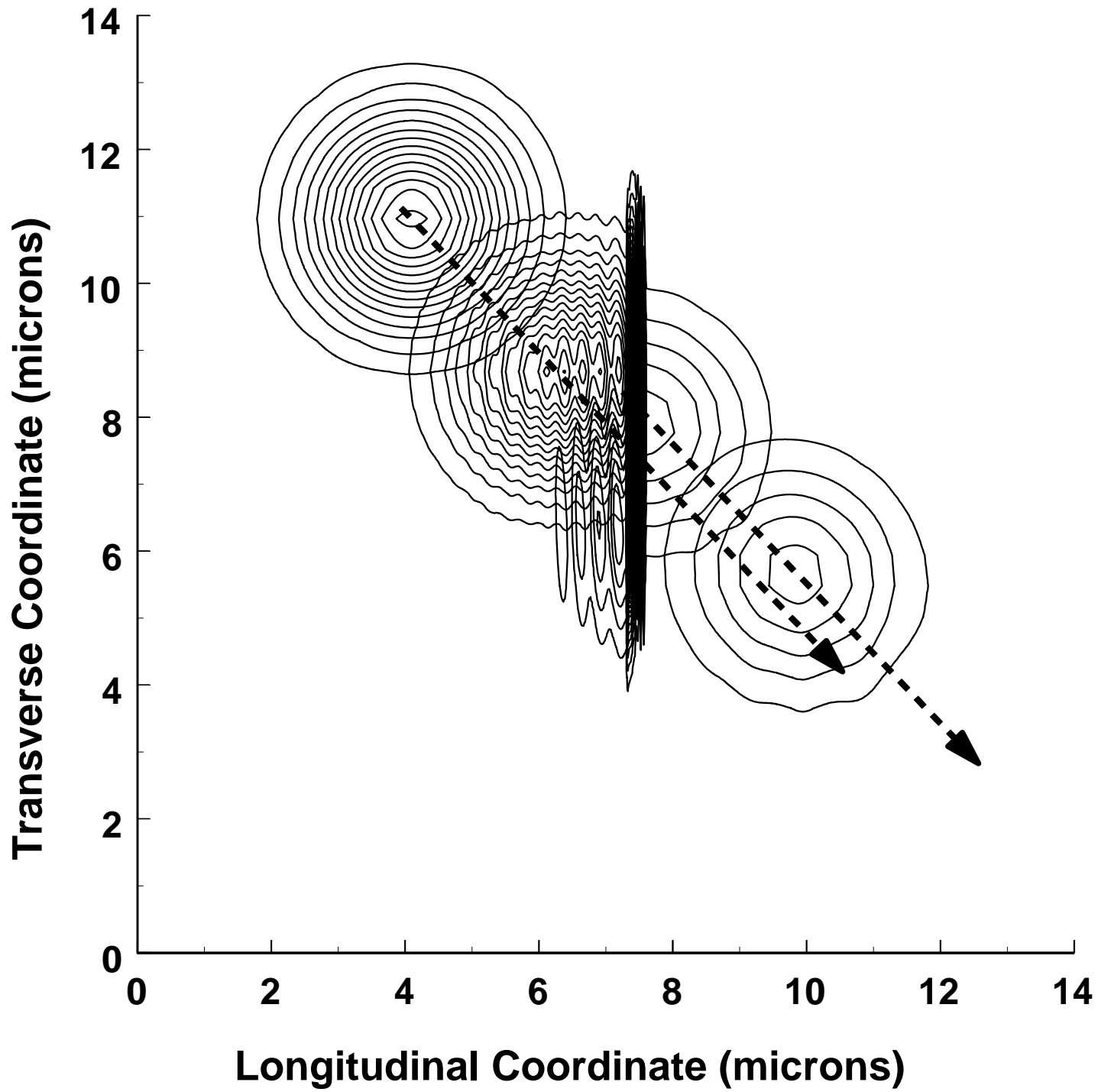


Fig.2

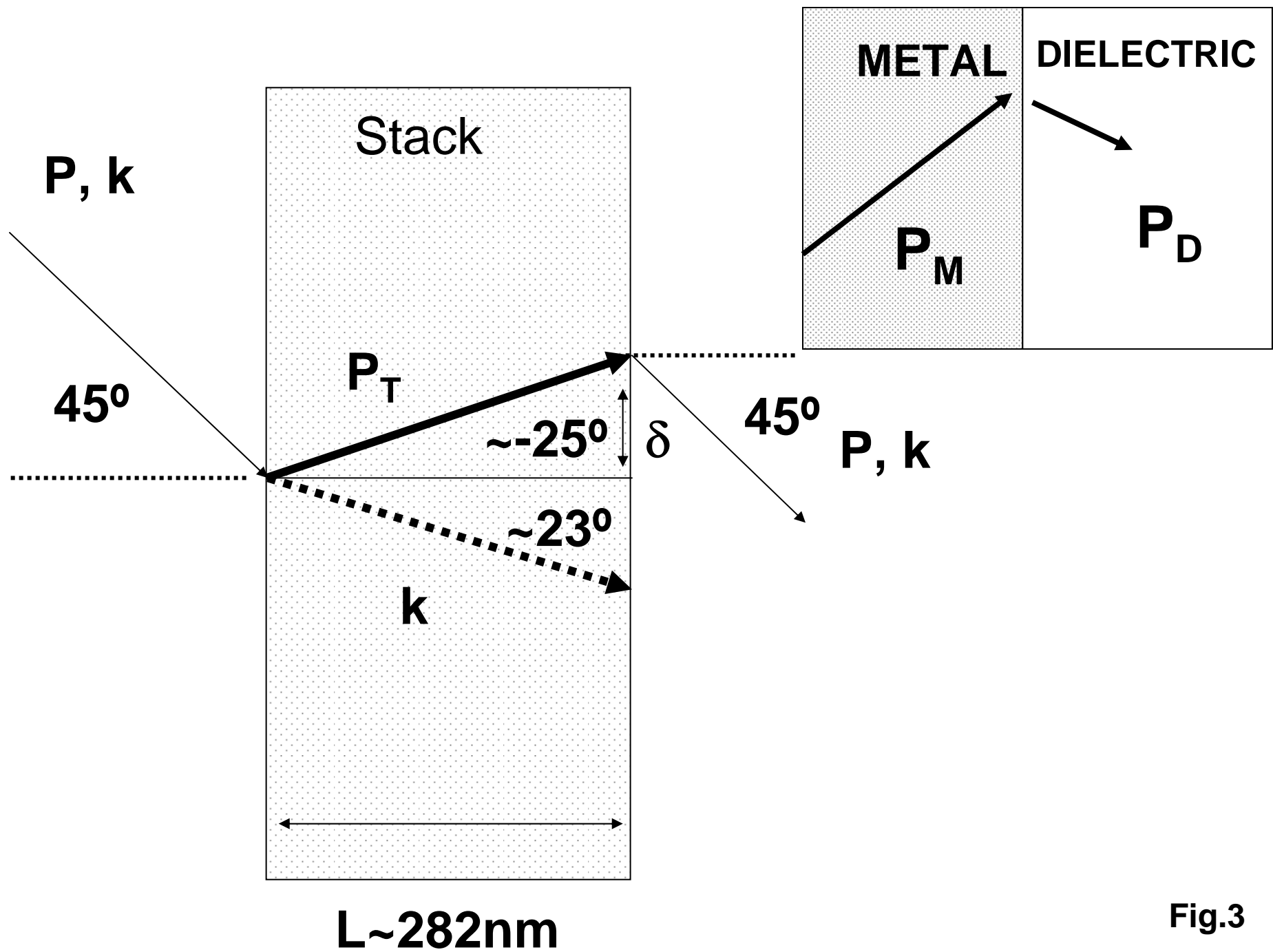


Fig.3

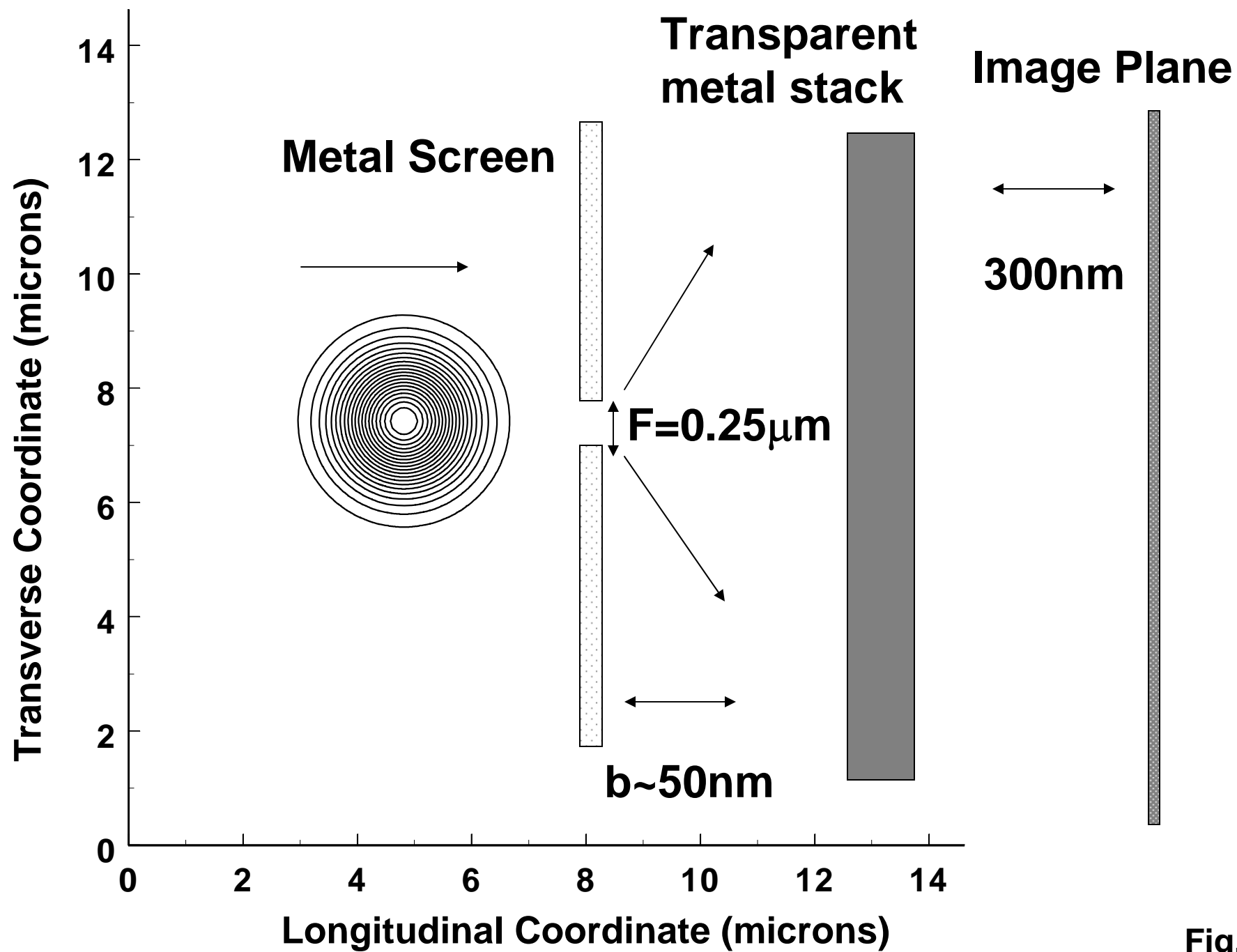
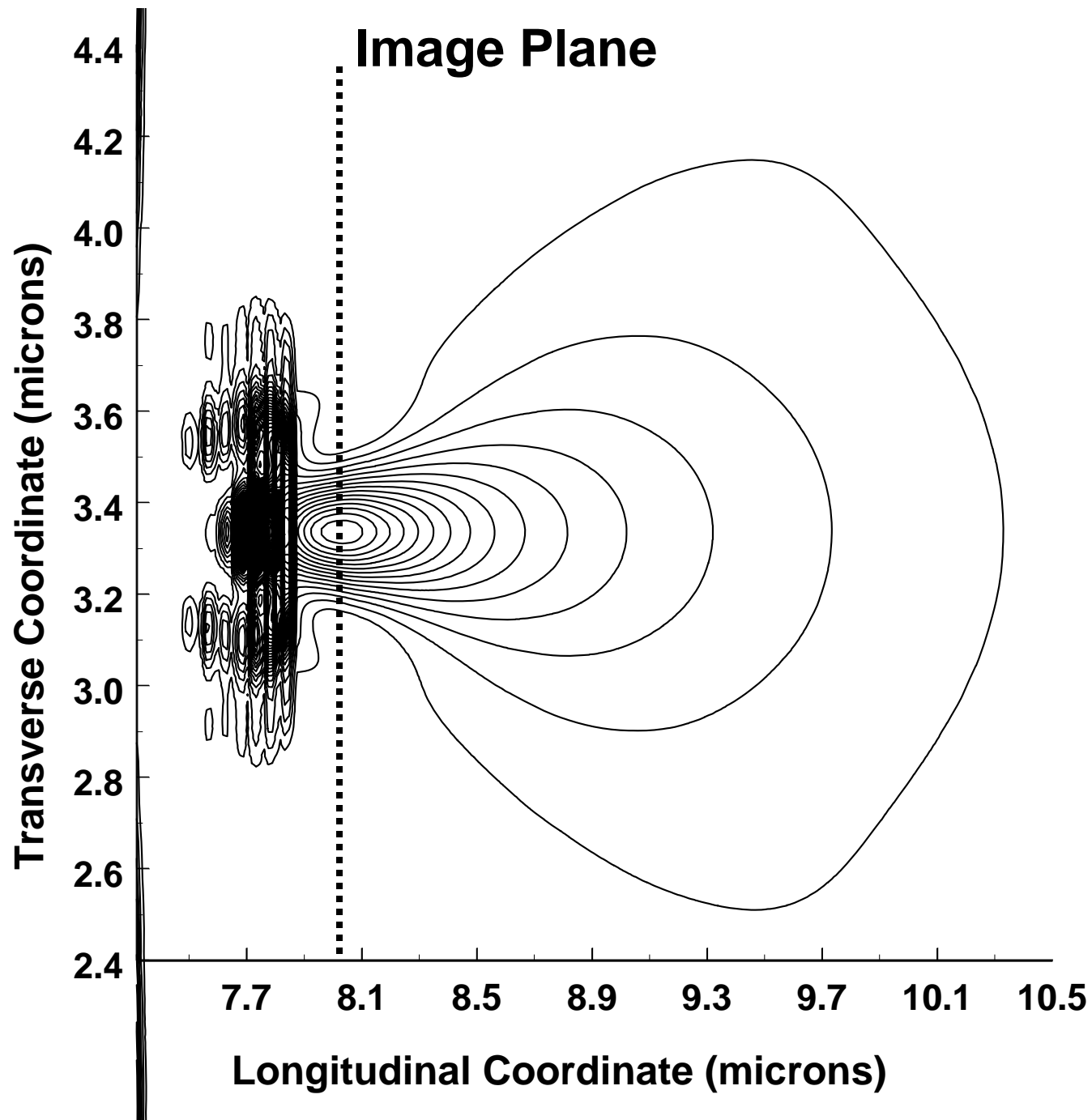
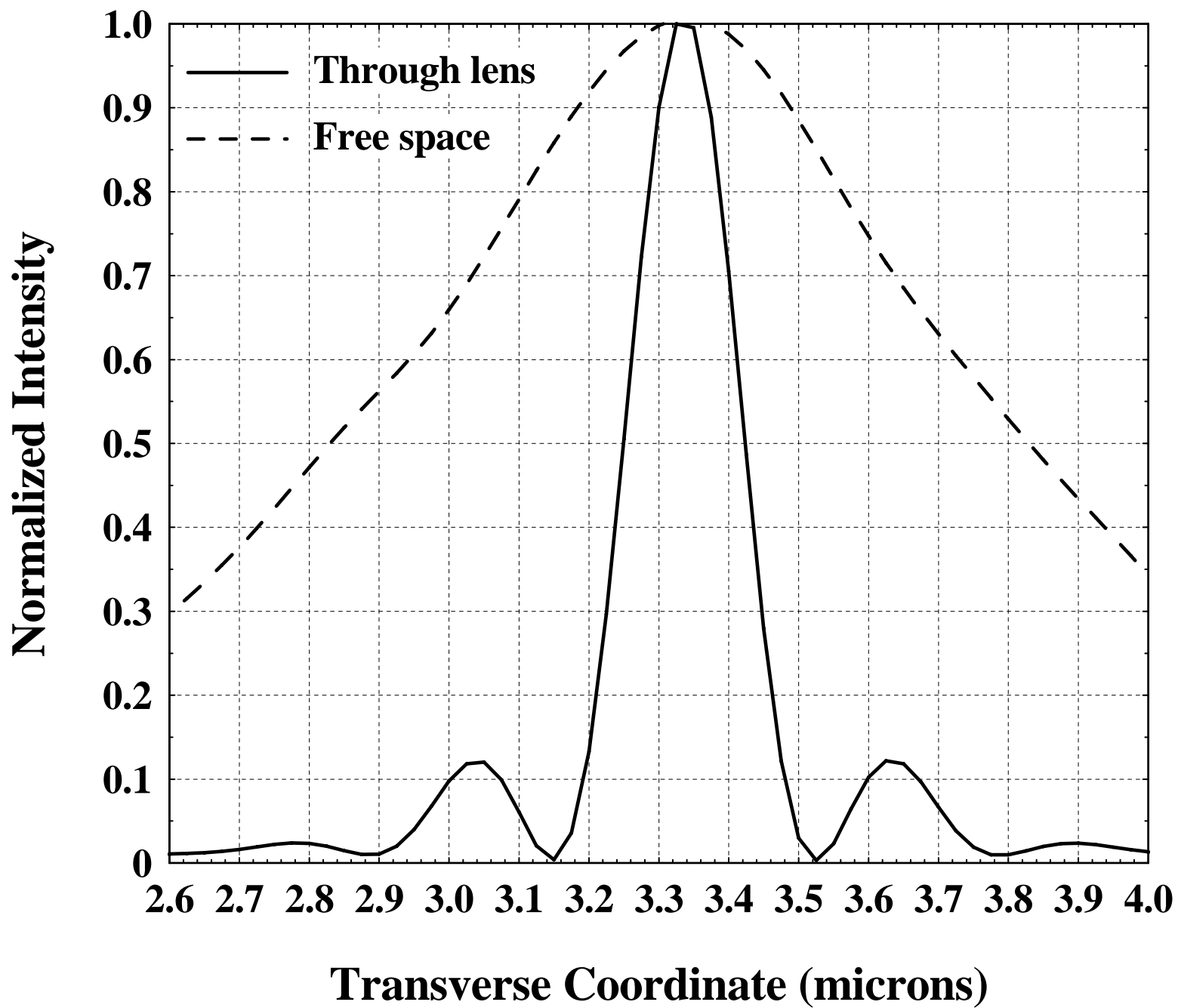


Fig.4



**Fig.5**



**Fig.6**